NJC

Accepted Manuscript

This is an *Accepted Manuscript*, which has been through the Royal Society of Chemistry peer review process and has been accepted for publication.

Accepted Manuscripts are published online shortly after acceptance, before technical editing, formatting and proof reading. Using this free service, authors can make their results available to the community, in citable form, before we publish the edited article. We will replace this *Accepted Manuscript* with the edited and formatted *Advance Article* as soon as it is available.

You can find more information about *Accepted Manuscripts* in the Information for Authors.

Please note that technical editing may introduce minor changes to the text and/or graphics, which may alter content. The journal's standard Terms & Conditions and the Ethical guidelines still apply. In no event shall the Royal Society of Chemistry be held responsible for any errors or omissions in this *Accepted Manuscript* or any consequences arising from the use of any information it contains.

ROYAL SOCIETY OF CHEMISTRY

www.rsc.org/njc

Journal Name

ARTICLE

Autonomous movement induced in chemically powered active soft-oxometalates using dithionite as fuel

Received 00th January 20xx,
Accepted 00th January 20xx

DOI: 10.1039/x0xx00000x

www.rsc.org/

Apabrita Mallick, Dipti Lai, Soumyajit Roy*

Synthesis of autonomously moving nano or micromotors is an immediate challenge in current nanoscience and nanotechnology. In this work we report a system based on soft-oxometalates (SOMs) which is very easy to synthesize and moves autonomously in response to chemical stimuli like that of a reducing agent-dithionite. The redox active Mo^{VI} sites of SOMs are used for oxidizing dithionite to generate SO_2 to propel the micromotors. We explain this motion qualitatively and also show how surface interaction, adsorption isotherm of the evolved gas influence power conversion efficiency of these micromotors.

Introduction

Synthesis of autonomously moving soft and active matter[1] is an immediate challenge for modelling biological phenomenon. In recent times, although, moving matter has been designed[2-5], their synthesis is tedious. Here we report a system based on soft-oxometalates[6,7](SOMs) which is very easy to synthesize and is used as a model system in our study. We now explore the current status in the field of micromotors.

The first well known synthetic motor[8] was prepared by Whitesides et al. in 2002 which used Pt catalyst to drive millimetre scale plastic disks. Synthetic motors in micro meter scale were prepared in 2004-2005[9,10]. These micromotors were bimetallic rods of Pt-Au[9] and Ni-Au[10] of length 2-3 μm which catalytically decomposed H_2O_2 to H_2O and O_2 and moved with a speed of ~10 μm s^{-1}. The movement of synthetic micromotors is controlled by artificial stimuli such as chemical fuel[11-15], magnetic field[16-18], electric field[19-21], ultrasonic sound[22] or light[23-25]. Thus the operation of micromotors is dependent on the source of energy consumption and accordingly they can be classified as bubble propelled[5,11-12] micromotors, self electrophoretically propelled[13-15] micromotors, magnetically driven[16-18] micromotors, electrically driven[19-21] micromotors, ultrasound propelled[22a,b] micromotors and light driven[23-25] micromotors. The movement[26] of active motors can be in the form of translation[9], rotation[10], delivery[27] or collective behaviour[24]. Chemically powered micromotors[12] are mainly propelled due to gas generated by the surface catalytic decomposition[9] of the fuel. Chemically propelled micromotors can be either bubble propelled[11] or self electrophoretically[5] propelled. The requirement of chemical fuels can be obviated by using micromotors which use physical sources for their energy requirement like magnetic micromotors[16] driven in a magnetic field that convert their rotary motion to axial translation. Biocompatible fuel free micromotors can also be obtained from ultrasonic acoustic waves[22]. In low Reynold's number regime, Brownian motion plays the dominating role and thus the autonomous movement of micro objects is restricted[26]. At microscale, interfacial forces dominate over inertia[28] which is exploited to devise micromotors.

Soft-charged metal oxide based structures, the soft-oxometalates[6] (SOMs) with metals in high oxidation state provide us with an opportunity of inducing autonomous movement in these SOMs. SOMs have also been moved using optical forces before by us[23]. Redox chemistry of SOM provides a possibility for generating a gas by the oxidation of a reductant which can act as a fuel and in turn propel the SOMs. Here we exploit this possibility. More precisely, we take the step of inducing autonomous movement in heptamolybdate SOMs with the help of chemical fuel dithionite. We ask is it possible to exploit the redox active Mo^{VI} sites on SOMs to generate SO_2 gas by oxidation of the reductant dithionite? We address this question here.

Results and discussion:

The chemistry of inducing motion in SOMs:

For our study, we choose dithionite as the fuel and metal oxide (oxomolybdate) as reacting surface. We note the SOMs are rod shaped in nature with their size in agreement from DLS and SEM (see Fig.1).

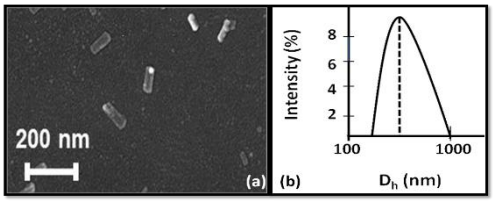

Fig.1 SEM image and **(b)** DLS size distribution plot of heptamolybdate SOMs.

EFAML, Materials Science Centre, Department of Chemistry, Indian Institute of Science Education and Research, Kolkata-741246
Email: s.roy@iiserkol.ac.in

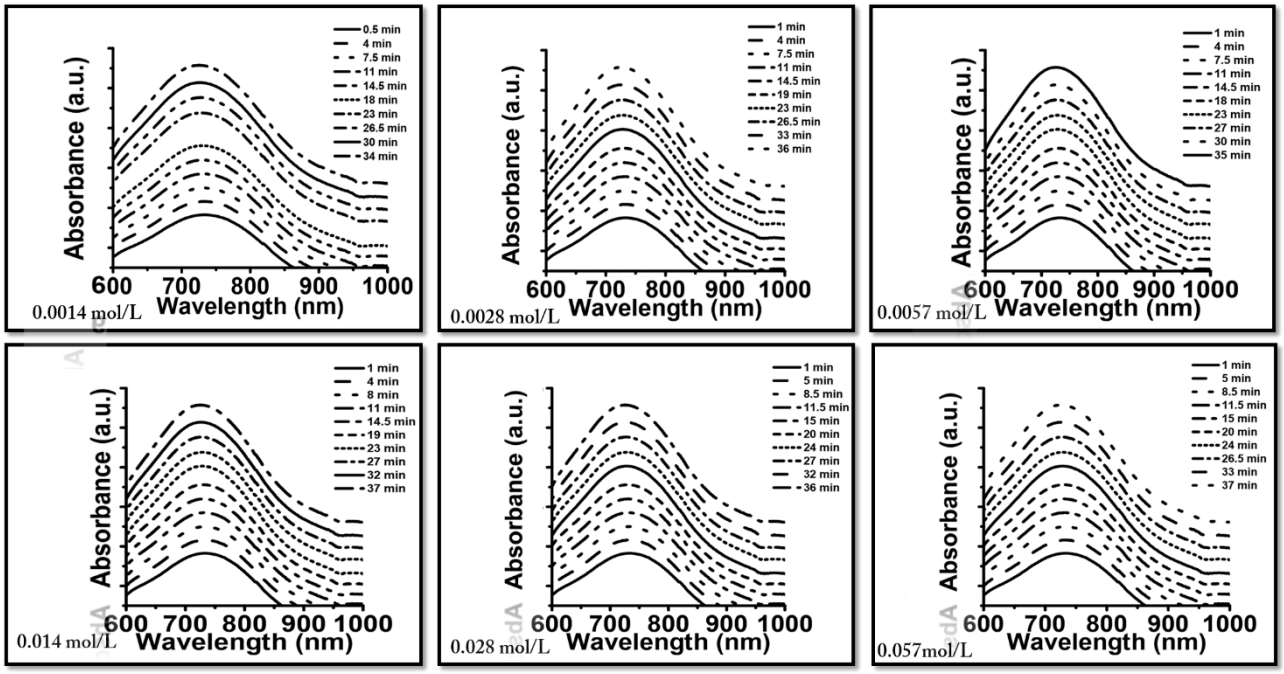

Fig.2 UV-visible spectra of SOM dithionite system at different concentrations of dithionite

Length of SOM rods from SEM is around 200 nm. In DLS the hydrodynamic diameter (D_h) is around 500 nm which is due to the tumbling motion of the rods that effectively gives rise to a sphere of 500 nm diameter.

The aqueous solution of sodium dithionite is unstable[29] and in aerobic and acidic conditions(under the conditions of autonomous movement shown by the SOMs) it generates sulphur and sulphur dioxide. So we used freshly prepared solution of sodium dithionite for our experiment.

When an aqueous solution of sodium dithionite ($Na_2S_2O_4$) is added to the dispersion of mildly acidic isopolyacids of SOMs, dithionite gets oxidised to SO_2 and Mo^{VI} centres of SOM get reduced to Mo^{V} centres which ultimately generate molybdenum blue type SOMs and propels the SOMs. Thus propulsion of SOMs is a result of a redox reaction which gives rise to a gaseous oxidized product SO_2 and a reduced molybdenum blue SOM which is blue in colour due to IVCT type transition ($Mo^{V} \rightarrow Mo^{VI}$).The SO_2 produced by the reaction of dithionite with heptamolybdate remains in the solution for considerable amount of time which in turn propel these active SOM motors. So, the lifetime of active SOMs is also quite significant, though not infinite. In this reaction Mo^{VI} oxidises[30] dithionite to SO_2 in accordance to the following reaction (shown schematically):

$$Mo^{VI}{}_7O_{24} + S_2O_4^{2-} \longrightarrow \text{Molybdenum Blue} + 2SO_2\,(g)$$

This redox process in fact causes the motion of the SOMs oxidizing the dithionite and reducing the SOMs. The propulsion of SOMs due to the oxidation of SO_2 is coupled with the reduction of SOMs and thus the emergence of $Mo^{V} \rightarrow Mo^{VI}$ intervalence charge transfer (IVCT) in the molybdenum blue SOMs; the extent of SO_2 evolution can hence be monitored by electronic absorption spectroscopy (Fig.2). The extent of SO_2 produced in the above reaction is coupled with the generation of blue SOMs which is signalled by the intensity $Mo^{VI} \rightarrow Mo^{V}$ IVCT band in blue SOMs. In this way we are able to find the extent of generation of SO_2 from electronic absorption spectroscopy and we plot the amount of SO_2 liberated against the loading variation of dithionite used for propelling the SOM micromotors (Fig. 3)."

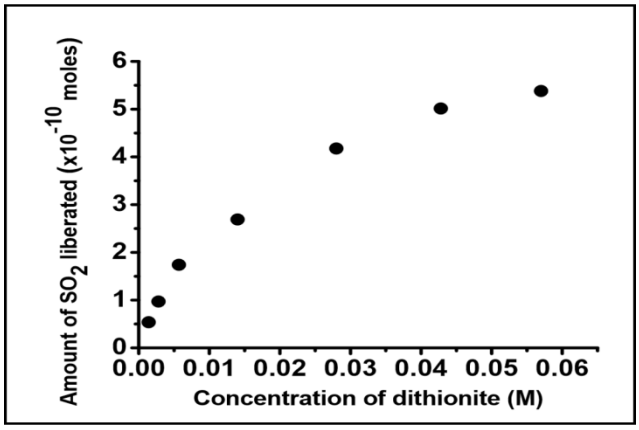

Fig. 3 Plot of amount of SO_2 liberated vs loading variation of dithionite

On the other hand motion is induced in SOMs (Fig.4, ESI†) due to the movement of the osmotic boundary between the reacting interface and the moving particle.To understand the effect of the fuel dithionite qualitatively, we load sodium dithionite of varying concentrations in the system. To analyse the individual movement of SOM particle we calculate the velocity of SOM at different concentrations of dithionite (Fig.5 (a) and also determine the trajectories using ImageJ and TrackPy[31] (Fig.5 (b)-(g)). The details of analysis are given in the experimental section.

The movement of SOMs in aqueous dispersion is entirely Brownian in nature. On addition of the fuel, reaction starts at the surface of

the SOM and it shows directed autonomous translation. With the increase in the concentration of the fuel, velocity of SOMs increases initially upto 52 body lengths s^{-1} (for 0.014 mol/L of sodium dithionite). But after that the velocity decreases even if the dithionite concentration is increased. At 0.0574 mol/L dithionite concentration the motion of SOMs is again Brownian in nature. Past 0.0574 mol/L we cannot track the movement of active SOMs because the colour of the dispersion becomes too dark (blue) for microscopic imaging. We demonstrate this graph of velocity of active SOMs and the trajectories in Fig.5.

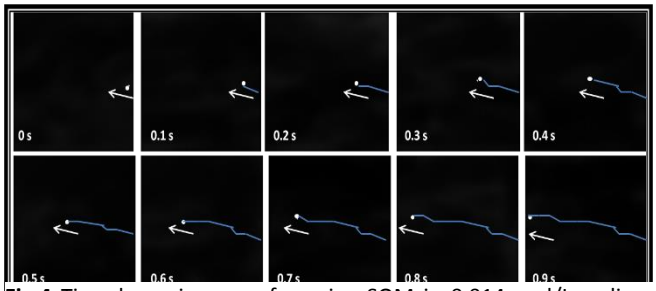

Fig.4 Time lapse images of moving SOM in 0.014 mol/L sodium dithionite. Direction of motion is shown by the arrow and the blue lines indicate the trace lines.

On the motion of SOMs: We now explain qualitatively the mechanism of the induced motion of SOMs. As the above reactions start, mobile diffuse boundary separating the starting SOM with the molybdenum blue type species' interface is generated. This interface generates an osmotic boundary. At this boundary SO_2 gas is produced due to which a slip velocity is created between the SOM interface and the continuous medium, which propels the SOMs.

As we increase the fuel concentration, more and more sodium dithionite react with SOMs, more SO_2 is produced. The thrust produced by the evolved gas on SOM increases. Consequently, SOM travels with increasing velocity till it reaches a tipping point. When more gas is evolved, more SO_2 molecules get adsorbed on the surface of the SOM. Thus the unreacted SOM interface now interacts with less amount of fuel and we observe decrease in velocity of SOMs. For sodium dithionite the tipping point is observed at 0.014 mol/L concentration. Beyond this concentration of 0.014 mol/L of sodium dithionite, we believe the SOM surface sites are all saturated and this creates an additional viscous drag and consequently velocity of SOMs drop. With further reaction, the osmotic boundary reaches equilibrium and there is no asymmetry between the osmotic boundary and the SOM surface. Thus the slip velocity decreases to near zero. Since all the reactions were carried out at a uniform temperature so we can plot adsorption isotherm by calculating the area of SOM occupied by adsorbed SO_2 where θ is the fraction of the surface that is covered with gaseous molecules, p is the pressure of SO_2 gas.

From the graph (Fig.6) it is evident that the fraction of occupied

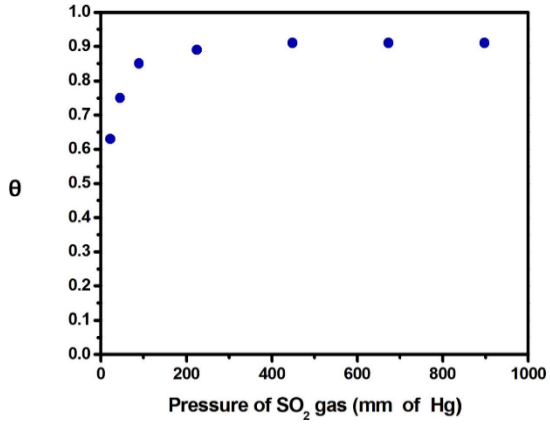

Fig.6 Adsorption isotherm of evolved SO_2 on the surface of SOMs

sites on active SOM surface increases with the increasing pressure of SO_2. On increasing concentration of dithionite, more SO_2 gas is produced and the pressure of SO_2 also increases as pressure is directly proportional to concentration. When all the active sites on SOM are occupied by the SO_2 gas θ reaches a saturation point.

We can describe the motion of SOMs using osmophoresis. In this model, for reaction rate dominated regime[32], average velocity of the particles is given by,

$$v = -\frac{\Gamma' k_\beta T \alpha_{eff}}{8\pi D R^2 \eta}$$

where Γ' is the reaction rate, $k_\beta T$ is the thermal energy, α_{eff} describes the interaction between the molybdenum blue formed and the unreacted SOM surface, D is the diffusivity, R is the hydrodynamic radius of the particle and η is the co-efficient of viscosity. α_{eff} is very small and lies in the range 0.12 nm^2 to 3.46 nm^2 (Table 1).

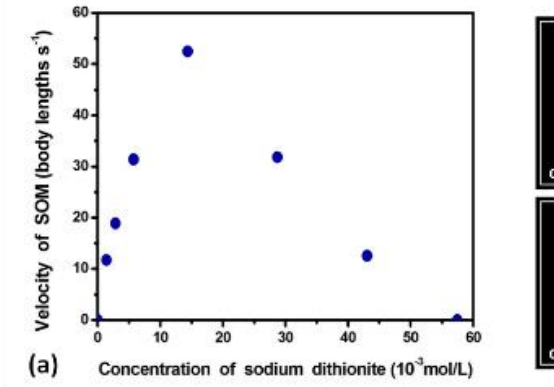

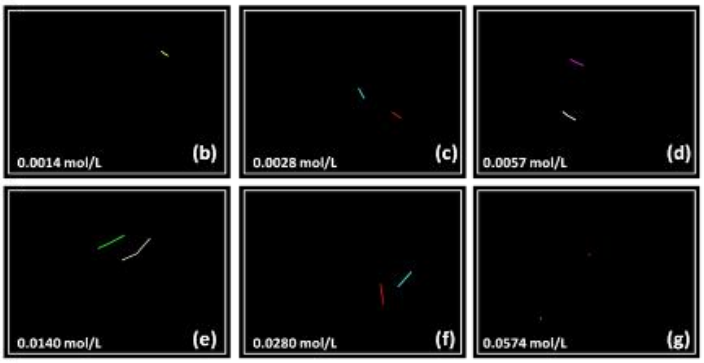

Fig.5 (a): Plot of velocity of SOM vs. concentration of sodium dithionite. **(b) – (g):** Trajectory pathways (shown by coloured lines for different SOM particles) of moving SOM in different dithionite concentrations for 1 second.

Concentration of sodium dithionite (mol/L)	α_{eff} (nm^2)
0.0014	3.46
0.0028	2.78
0.0057	2.31
0.0140	1.54
0.0280	0.46
0.0430	0.12

Table.1 Surface interaction between the product of catalytic decomposition and SOM surface.

O**n power conversion efficiency:** The power conversion efficiency[33] of these micromotors can be defined as:

$$\eta = \frac{P_{mech}}{P_{chem}}$$

where P_{mech} is the mechanical energy output and is given by $P_{mech} = F_{drag} v = f v^2$
and P_{chem} is the chemical energy input and is given by $P_{chem} = n\Delta_r G$.
For cylinders, $f = \frac{2\pi\mu L}{\ln\left(\frac{L}{R}\right) - 0.72}$.

Here F_{drag} is the drag force on the cylindrical SOM, f is the drag coefficient, μ is the dynamic viscosity of water, L is the length of SOM, R is its radius, υ is the motor speed, n is the gas evolution rate in units of mol/(SOM·s) and $\Delta_r G$ is the Gibbs free energy of the decomposition of dithionite. We calculate the values of P_{mech} and P_{chem} and find the energy efficiency of SOM micromotors in the following table (Table 2).

Concentration of sodium dithionite (mol/L)	P_{mech} (Joules)	P_{chem} (Joules)	Efficiency(η)
0.0014	2.14×10^{-22}	8.58×10^{-13}	2.49×10^{-10}
0.0028	5.56×10^{-22}	1.71×10^{-12}	3.25×10^{-10}
0.0057	7.15×10^{-22}	3.43×10^{-12}	2.08×10^{-10}
0.0140	4.30×10^{-21}	8.58×10^{-12}	5.01×10^{-10}
0.0280	1.58×10^{-21}	1.71×10^{-11}	9.29×10^{-11}
0.0430	2.45×10^{-22}	2.57×10^{-11}	9.53×10^{-12}

Table.2 Power conversion efficiency of the SOM micromotors in SOM-dithionite system

The power conversion efficiency (Fig. 7) of SOM micromotors using dithionite as the fuel varies in the order of 10^{-12} to 10^{-10}. The maximum efficiency is observed to be 5.01×10^{-10} for 0.014 mol/L dithionite where the velocity of these SOM particles is also maximum.

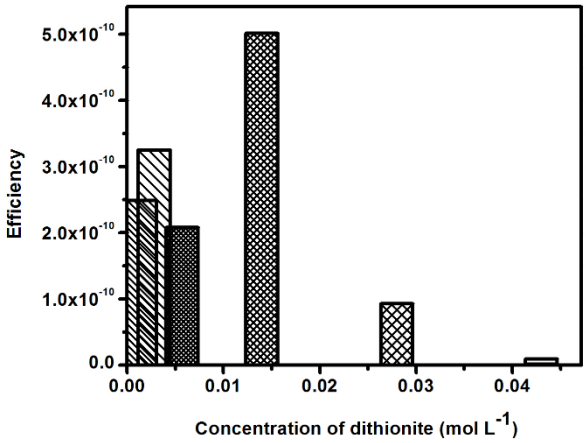

Fig.7 Power conversion efficiency of SOM micromotors at different dithionite concentrations.

Conclusion:

To conclude, using molybdenum based soft-oxometalates (SOMs) and employing sodium dithionite as a fuel, we can make SOMs move. The motility in SOMs stems from the evolution of the SO_2 gases by the oxidation of dithionite to SO_2 with concomitant reduction of Mo_7-SOMs to molybdenum blue type SOMs. The reaction creates an osmotic boundary between the newly generated product (including the gas) and the unreacted reactant SOM surface. The chemical potential gradient between the SOM surface and reactive osmotic interface (with evolving gas) gives rise to a slip velocity to the SOMs propelling them. The velocity of SOMs increases upto a certain limit (52 body lengths s^{-1}) till the SOM surface is saturated with evolved gases as seen from adsorption isotherm. At such saturation value, the SOM velocity reaches a maximum of 52 body lengths s^{-1} and due to the viscous drag induced by the evolved gases on the SOM surface, the velocity decreases and finally drops to zero, when the viscous drag annuls the slip velocity. This explains that using a simple redox system and exploiting this potential in SOMs it is possible to construct SOM micromotors and in principle possibilities exist for fine tuning their motion. The high propulsion velocity and facile synthesis of heptamolybdate SOM hold considerable importance in the field of active matter and can be used in future for cargo transport[34], catalysis[35] and drug release[36]. A more quantitative understanding of this phenomenon using other model systems is currently under investigation in our laboratory.

Experimental details:

Preparations:
The reagents were purchased from commercial sources (Merck) and used without further purification. The glassware was cleaned in an acid bath, base bath and rinsed with isopropanol followed by acetone and kept in an oven for 48 hours prior to use.
Synthesis of Ammonium heptamolybdate soft oxometalate (SOM): Ammonium heptamolybdate tetrahydrate (1500 mg, 1.213

mmol) was dissolved in distilled water (4 mL) and heated until simmering hot. A clear dispersion of ammonium heptamolybdate was formed, which was then stored in a refrigerator for 10 minutes. The dispersion was brought to room temperature which scattered light from laser.

Synthesis of sodium dithionite solutions: Calculated amount of sodium dithionite was dissolved in 10mL of distilled water to prepare dithionite solutions of concentrations 0.0014 mol/L, 0.0028 mol/L, 0.0057 mol/L, 0.0140 mol/L, 0.0280 mol/L, 0.0430 mol/L and 0.0574 mol/L.

Instrumental Analysis:

Microscopy using inverted fluorescence microscope: An Olympus IX81epi fluorescence microscope with a motorized stage was used for recording videos. A 22X40 cover slip was cleaned with methanol and dried to remove any unwanted adsorbed material. The SOM dispersion (10 µL) was placed on that cover slip. The cover slip was then placed on the microscope scanning stage and the stage was controlled using a joystick. 10 µL of sodium dithionite solution (of known concentration) was added to the SOM dispersion using a 10 µL micropipette. The dispersion which was initially colourless turned blue on addition of dithionite. The microscope was focused at 40X objective and the videos were recorded using DSIC camera at a rate of 10 frames per second.

Characterisation using Scanning Electron Microscopy (SEM): The SEM image was taken on SUPRA 55 VP-41-32 instrument with the SmartSEM version 5.05 Zeiss software.

Characterisation using Dynamic Light Scattering (DLS) measurement: 0.5 mL of heptamolybdate SOM dispersion was diluted with 10 mL of deionised water. This dispersion was irradiated with a hand held laser pointer of wavelength 635 nm which resulted in the scattering of a single well-defined line. The resulting dispersion was then subjected to DLS experiment using Malvern Zetasizer.

Image Analysis:

Analysis with ImageJ: The raw image sequence in .TIFF format was converted to .AVI form using ImageJ. From these videos each frame was separately taken and the SOM particles in that frame were analysed manually. That is, the co-ordinates of position of a SOM particle was measured over 3 frames, the body length of that particular SOM was taken into account (as SOMs are of varying size), time gap between the frames was noted and using these velocity of each SOM was calculated. This procedure was repeated for a number of SOMs in each video corresponding to a particular dithionite concentration. The average of these velocities was considered as the velocity of the SOM at that particular dithionite concentration. The same procedure was carried out for all dithionite concentrations. The velocities of SOM were plotted in a graph against concentration of sodium dithionite.

Analysis with Trackpy: Trackpy is a python packaging tool used for particle tracking. Using this code each video was analysed and trajectories of SOM were obtained. Trackpy first identified SOM particles in each frame with selective filters in it and then connected the frames in which a SOM particle was present to obtain the particle trajectories. For each dithionite concentration code was written separately and particle trajectories were obtained.

Acknowledgement:

SR gratefully acknowledges the grants from IISER-Kolkata, India, DST-fast track, BRNS-DAE grant, Mr. Ritabrata Ghosh for helping with the imaging and Mr. Abhrajit Laskar (IMSc, Chennai) for his help and support.

References:

1 S. Ghose and R. Adhikari, *Physical review letters*, 2014, **112**, 118102.
2 S. Sengupta, D. Patra, I. Ortiz-Rivera, A. Agrawal, S. Shklyaev, K. K. Dey, U. Córdova-Figueroa, T. E. Mallouk and A. Sen, *Nature chemistry*, 2014, **6**, 415-422.
3 J. Li, W. Gao, R. Dong, A. Pei, S. Sattayasamitsathit and J. Wang, *Nature communications*, 2014, **5**, 5026.
4 K. Kim, X. Xu, J. Guo and D. Fan, *Nature communications*, 2014, **5**, 3632.
5 S. Sanchez, A. N. Ananth, V. M. Fomin, M. Viehrig and O. G. Schmidt, *Journal of the American Chemical Society*, 2011, **133**, 14860-14863.
6 S. Roy, *CrystEngComm*, 2014, **16**, 4667-4676.
7 S. Roy, *Comments on Inorganic Chemistry*, 2011, **32**, 113.
8 R. F. Ismagilov, A. Schwartz, N. Bowden, G. M. Whitesides, *Angewandte Chemie,* 2002, **114**, 674-676.
9 W. F. Paxton, K. C. Kistler, C. C. Olmeda, A. Sen, S. K. St. Angelo, Y. Cao, T. E. Mallouk, P. E. Lammert and V. H. Crespi, *Journal of the American Chemical Society*, 2004, **126**, 13424-13431.
10 S. Fournier-Bidoz, A. C. Arsenault, I. Manners and G. A. Ozin, *Chemical Communications*, 2005, **4**, 441-443.
11 J. Wang and W. Gao, *ACS nano*, 2012, **6**, 5745-5751.
12 W. Gao, S. Sattayasamitsathit, J. Orozco and J. Wang, *Journal of the American Chemical Society*, 2011, **133**, 11862-11864.
13 S. Sattayasamitsathit, W. Gao, P. Calvo-Marzal, K. M. Manesh and J. Wang, *ChemPhysChem*, 2010, **11**, 2802-2805.
14 R. Laocharoensuk, J. Burdick and J. Wang, *ACS nano*, 2008, **2**, 1069-1075.
15 N. S. Zacharia, Z. S. Sadeq and G. A. Ozin, *Chemical Communications*, 2009, **39**, 5856-5858.
16 L. Zhang, T. Petit, Y. Lu, B. E. Kratochvil, K. E. Peyer, R. Pei, J. Lou and B. J. Nelson, *ACS nano*, 2010, **4**, 6228-6234.
17 A. Ghosh and P. Fischer, *Nano letters*, 2009, **9**, 2243-2245.
18 S. Tottori, L. Zhang, F. Qiu, K. K. Krawczyk, A. Franco-Obregón and B. J. Nelson, *Advanced materials*, 2012, **24**, 811-816.
19 G. Loget and A. Kuhn, *Journal of the American Chemical Society*, 2010, **132**, 15918-15919.
20 P. Calvo-Marzal, S. Sattayasamitsathit, S. Balasubramanian, J. R. Windmiller, C. Dao and J. Wang, *Chemical Communications*, 2010, **46**, 1623-1624.
21 S. T. Chang, V. N. Paunov, D. N. Petsev and O. D. Velev, *Nature Materials*, 2007, **6**, 235-240.
22 (a) V. Garcia-Gradilla, J. Orozco, S. Sattayasamitsathit, F. Soto, F. Kuralay, A. Pourazary, A. Katzenberg, W. Gao, Y. Shen and J. Wang, *ACS nano*, 2013, **7**, 9232-9240.

(b) Z. Wu, T. Li, J. Li, W. Gao, T. Xu, C. Christianson, W. Gao, *ACS Nano*, 2014, **8**, 12041.

23 B. Roy, A. Sahasrabudhe, B. Parasar, N. Ghosh, P. Panigrahi, A. Banerjee and S. Roy, *Journal of Molecular and Engineering Materials*, 2014, **2**, 1440006.

24 M. Ibele, T. E. Mallouk and A. Sen, *Angewandte Chemie International Edition*, 2009, **48**, 3308-3312.

25 Z. Wu, X. Lin, Y. Wu, T. Si, J. Sun, Q. He, *ACS Nano,* 2014, **8,** 6097.

26 M. Guix, C. C. Mayorga-Martinez and A. Merkoçi, *Chemical reviews*, 2014, **114**, 6285-6322.

27 S. Sattayasamitsathit, H. Kou, W. Gao, W. Thavarajah, K. Kaufmann, L. Zhang and J. Wang, *Small*, 2014, **10**, 2830-2833.

28 T. R. Kline, W. F. Paxton, T. E. Mallouk and A. Sen, *Angewandte Chemie*, 2005, **117**, 754-756.

29 Burlamacchi, L.; Guarini, G.; Tiezzi, E. *Transactions of the Faraday Society,* 1969, **65**, 496.

30 A. Muller, K. Das, E. Krickemyer, and C. Kuhlmann, *Inorganic synthesis*, 2004, **34,** 191-200.

31 D.B. Allan, T.A. Caswell, N.C. Keim, Trackpyv0.2.ZENODO, 2014. DOI:10.5281/zenodo.9971.

32 A. Brown and W. Poon, *Soft matter*, 2014, **10**, 4016-4027.

33 W. Wang, T.-Y. Chiang, D. Velegol and T. E. Mallouk, *Journal of the American Chemical Society*, 2013, **135**, 10557-10565.

34 L. L. del Mercato, M. Carraro, A. Zizzari, M. Bianco, R. Miglietta, V. Arima, I. Viola, C. Nobile, A. Sorarù and D. Vilona, *Chemistry-A European Journal*, 2014, **20**, 10910-10914.

35 J. Li, V. V. Singh, S. Sattayasamitsathit, J. Orozco, K. Kaufmann, R. Dong, W. Gao, B. Jurado-Sanchez, Y. Fedorak and J. Wang, *ACS nano*, 2014, **8**, 11118-11125.

36 Z. Wu, Y. Wu, W. He, X. Lin, J. Sun, Q. He, *Angew. Chem., Int. Ed.,* 2013*,* **52***,* 7000.

Micromotors based on Mo_7 soft-oxometalates (SOMs) which is very easy to synthesize and moves autonomously in presence of dithionite which acts as the chemical fuel.